Particle recirculation studies in JET

E. Tsitrone, J. Bucalossi, T. Loarer, Ph. Ghendrih, A. Loarte[a], P. Andrew [b], P. Coad [b], W. Fundamenski [b], M. Stamp [b], D. Coster [c] and contributors to the JET EFDA work programme

Association EURATOM-CEA, DRFC, CEA Cadarache, 13108 St Paul lez Durance, France

[a] EFDA CSU Garching, Max Planck Institut für Plasmaphysik, D-85748 Garching, Germany

[b] UKAEA- Euratom Fusion Association, Abingdon, Oxfordshire OX14 3EA, UK

[c] Max Planck Institut für Plasmaphysik, IPP Euratom Assoziation, D-85748 Garching, Germany

Abstract

A global particle balance analysis has been applied to a variety of L mode and H mode deuterium discharges of the C4 campaign of JET, performed at a lower wall temperature, in different magnetic configurations and with various divertor gas puffing location. Wall retention and divertor particle exhaust are discussed as a function of the plasma configuration, the wall temperature and the gas puffing location. The effect on ELMs frequency is also mentioned. A simple empirical law linking the divertor pressure and the Dα signal integrated on the divertor is derived.

1 Introduction

Control of particle recirculation at the plasma boundary is a key element in the demonstration of the capability of any divertor to achieve high performance. In the present analysis, this issue is tackled from the viewpoint of gas injection efficiency, relationship between pumping, particle recirculation and wall particle trapping. All three issues affect strongly plasma operation, with impact on building up the core density, determining optimised pumping schemes, preventing density slide-away due to wall saturation as well as controlling the tritium inventory [1]. In the first section, a global particle balance analysis, allowing to evaluate the dynamic wall retention, is described. This analysis is then applied to a variety of L mode and H mode deuterium discharges of the C4 campaign, performed at lower wall temperature on JET during january 2001. Different magnetic configurations and various divertor gas puffing locations are compared, in order to gain insight on the neutral recirculation pattern. In the second section, the divertor performance in terms of particle exhaust is examined in more details.

2 Particle balance

2.1 Description of the particle balance analysis

Particle recirculation has been studied through a global particle balance analysis, using the methodology described in [2]. The global particle balance can be written as follows, simply stating that all particles injected in the machine go either in the plasma, in the pumping systems or in the wall :

$$\int_0^t Q_{inj}dt = <n_e>V_p + \int_0^t Q_{pump}dt + N_{wall} \qquad (1)$$

where :

- Q_{inj} is the total particle injection rate in the machine ($Q_{inj} = Q_{gas} + Q_{NBI} + Q_{pellet}$, where Q_{gas}, Q_{NBI}, Q_{pellet} are the injection rates associated respectively with gas puffing, neutral beam injection and pellet injection),
- $<n_e> V_p$ is the total number of particle in the plasma, $<n_e>$ being the volume averaged density and V_p the plasma volume,
- Q_{pump} is the total rate of particle extracted by the pumping systems of the machine ($Q_{pump} = Q_{div}+Q_{ves}$ where Q_{div} is the particle rate extracted by the divertor cryopump and Q_{ves} is the particle rate extracted by the vessel and the neutral beam boxes pumps.) The extracted rates are calculated as follows : $Q_{div} = P_{subdiv} \times S_{div}$ where P_{subdiv} is the subdivertor neutral pressure (KT5P pressure gauge) and S_{div} the associated pumping speed, determined as described in [2], with different values depending on the plasma configuration (for deuterium, $S_{div} = 110$ m^3s^{-1} when the plasma is in a X point configuration and $S_{div} = 250$ m^3s^{-1} otherwise). $Q_{ves} = P_{ves} \times S_{ves}$ where P_{ves} is the vessel mid plane neutral pressure and S_{ves} the associated pumping speed including the neutral beam boxes cryopumps and the vessel turbopumps (for deuterium, $S_{ves} = 89$ m^3s^{-1}) [1].
- N_{wall} is the total number of particle trapped in the walls of the machine.

All the above quantities (injection rates, plasma density and volume, neutral pressures and pumping speeds) are estimated from experimental measurements, except the wall content, which is deduced from the quoted experimental measurement using (1).

[1] It has to be noted that the pumping speeds values used here to analyse the C4 campaign shots with a lower wall temperature (T_{wall} = 200 °C instead of 320 °C) have been taken to be the same as in the previous campaigns. This

This analysis has been applied to a variety of deuterium discharges (L mode and H mode, gas puffing from various Gas Injection Modules (GIMs), different magnetic configurations) to gain insight on particle recirculation patterns.

2.2 Description of the database

The database include the following deuterium shots obtained during the C4 campaign, performed from january to march 2001 at lower wall temperature (T_{wall} = 200 °C instead of 320 °C) :

* H mode shots :
  - 12 MW shots in corner, lower vertical and upper vertical configurations, with 2 successive gas puffing phases with GIM9 (outer divertor base) and GIM11 (inner divertor base). Gas fuelling slightly higher for GIM9 (2.3 10^{22} e/s instead of 1.9 10^{22} e/s for GIM11) to compensate for loss in the cryopump (3 shots).
  - 15 MW shots in ITER like and lower delta configurations, with 1 gas puff either by GIM9 (outer divertor base), GIM10 (outer divertor ring) or GIM11 (inner divertor base). Same gas fuelling for all discharges (2 10^{22} e/s) (6 shots)

* L mode shots :
  - 4 MW shots in corner, lower vertical and upper vertical configurations, with 2 successive gas puffing phases with GIM9 (outer divertor base) and GIM11 (inner divertor base) :). Gas fuelling slightly higher for GIM9 (2.3 10^{22} e/s instead of 1.9 10^{22} e/s for GIM11) to compensate for loss in the cryopump (3 shots).
  - 2 MW density limit shots in high clearance 5 cm or high clearance 22 cm configuration, with gas puffing either by GIM9 and GIM 10 (outer divertor base and ring), GIM11 (inner divertor base) or GIM6 (main chamber). Gas fuelling is raised until the density limit is reached. (8 shots) [3]

Last, 2 shots of the above database have been compared with similar shots obtained previously with a higher wall temperature (ITER like and lower delta H mode with GIM11 fuelling).

The different magnetic configurations studied are shown in Figure 1, the locations of the divertor gas injection valves are shown on Figure 2.

---

is consistent with dry runs analysis, pressure drop in the vessel after the end of the shot, and cryopump regeneration data.

2.3 Discussion

The analysis described in section 2.1 is applied to the above database, from t = 39.5 s just before the plasma breakdown until t = 90 s (corresponding to the duration of the vessel neutral pressure measurements, 10 to 30 s after the end of the shot). Different inventories are followed :

- $N_{inj} = \int_0^t Q_{inj} dt$ is the injected particle inventory,
- $N_{pla} = \langle n_e \rangle V_p$ is the plasma inventory,
- $N_{div} = \int_0^t Q_{div} dt$ is the particle extracted by the divertor inventory,
- $N_{ves} = \int_0^t Q_{ves} dt$ the particle extracted by the vessel inventory,
- N_{wall} is the wall inventory, deduced from the others using (1).

All the above inventories are set to zero at the beginning of the shot, including N_{wall}, whose meaning here is rather the variation of the wall inventory during the discharge than an absolute value.

We can then define the associated fractions :

$\chi_{pla} = N_{pla}/N_{inj}$; $\chi_{div} = N_{div}/N_{inj}$; $\chi_{ves} = N_{ves}/N_{inj}$; $\chi_{wall} = N_{wall}/N_{inj}$

Figure 3 presents the balance reached at the end of the shot (t = 90 s) for the database (except the density limit shots), in terms of the fractions χ_{div} and χ_{wall} as a function of the subdivertor neutral pressure, which is a figure of merit of the divertor pumping performance. The pressure measurement is averaged over a stable plateau during the different gas injection phases. The fraction of particles extracted by the divertor increases with the measured divertor pressure (from 20-30% up to 40-50%), which shows that the balance reached after the shot is sensitive to the divertor performance during the gas injection phase. The fraction of particles extracted by the vessel is always modest (1 to 8%), but is in general slightly higher when the divertor is less efficient (higher neutral pressure in the main chamber). This leads to a wall retention from 50% to 70%. Although the variations on the different fractions are quite tenuous, a few comments can de drawn.

2.3.1 Comparison of H mode / L mode

In a given configuration, the wall retention of H mode shots is in general quite similar to the one of the L mode shots, except for the corner configuration where the wall retention is reduced in H Mode. Gas injection by the neutral beams represents 7 to 8% of the gas injection by the GIMs in H mode, while it is around 1.5 % in L mode. The plasma inventory is much higher in H mode than in the corresponding L mode shots, but it is not possible with the present analysis to distinguish between the effect of the better fuelling efficiency of the neutral beams and the improved particle confinement properties.

2.3.2 Effect of wall temperature

The two shots with high wall temperature (320°C instead of 200°C) included in the database (ITER like and lower delta H mode) exhibit a decreased wall retention (around 50 %) compared to the similar lower wall temperature shots. This is consistent with the general trend identified in [2] for the increased long term retention during the C4 campaign, and the fact that the wall reservoir should trap more particles at a lower surface temperature. Moreover, although the subdivertor and the main chamber pressure are quite similar for hot and cold walls, the private flux region (PFR) neutral pressure (measured from the PG23 pressure gauge, located on the outer side of the divertor septum) is twice as high for the hot walls. This effect can not be entirely attributed to the wall temperature change. Indeed, if one assumes that the neutrals are thermalised at the divertor target temperature (220°C for hot walls, 140°C for cold walls [3]), the temperature change would correspond to a factor 1.2 in the pressure.

Last, the shots with a lower wall temperature present a higher ELM frequency and a lower averaged density for the same gas injection (see Table 1). This effect has been reported on other shots in the ITER like configuration for medium fuelling (around 2 10^{22} part s^{-1}) but disappears at low and high fuelling as shown in Figure 4 [5].

2.3.3 Effect of the configuration

In terms of wall retention, the best results have been obtained with the corner and the lower delta H mode configurations (wall retention around 50%), where the divertor pumping is the most efficient (see subdivertor pressure in Figure 7). The ITER like configuration is the least favorable, specially with GIM9 outer fuelling (73% of retention), due to a poorer pumping by the divertor.

2.3.4 Effect of gas puff location

· GIMs location

This effect is complex to analyse because it is also closely linked to the plasma in/out asymmetry. Outer divertor gas injection generally leads to a lower fuelling efficiency during the plasma phase, as has been already reported in [4] , and a higher wall retention at the end of the shot. This is the case for most configurations, in particular for the density limit shots, where it is necessary to use both GIM9 and GIM10 to reach the density limit with outer fuelling. For these shots, wall retentions as high as 77% are reached with outer fuelling, while it is around 60% with inner or main chamber fuelling. The total number of injected particles necessary to reach the density limit is also quite different, in general twice as high with outer fuelling (3 to 4 10^{23} particles for GIM9+GIM10, depending on the configuration) while it is equivalent for the main chamber and inner fuelling (1.5 to 2 10^{23} for GIM11, GIM12 or GIM6 (main chamber)).

· In/out asymmetries

Strong in/out asymmetries are observed in the divertor plasma, as already stated in [4] for the corner and vertical target configurations. In particular, the inner divertor tends to detach earlier than the outer divertor [3][4] . Strong asymmetries in the D_α signal integrated on the inner ($D\alpha_{in}$) and outer ($D\alpha_{out}$) divertor are observed (see Figure 5, lower curve).

The gas puff location seems to play a role in the level of asymmetry only in closed divertor configurations, where the inner and the outer plasma are efficiently separated by the septum. For example, in the corner configuration, the asymmetry is strongly reduced when puffing from the outer divertor, while this effect is not seen in more open configurations such as the upper vertical target, but also the ITER like or the lower delta configurations. However, in all cases, $D\alpha_{in}$ is always stronger than $D\alpha_{out}$, even when gas puffing is performed from the outer divertor. The effect of the septum as a source of additional asymmetry has already been reported in [4] , where simulations of the divertor plasma in the corner configuration using the Edge2D-Nimbus code package show that removing the septum reduces the in/out detachment asymmetry (see also [8]).

In the studied L mode discharges, asymmetries up to $D\alpha_{in}.= 10\ D\alpha_{out}$ are observed. When looking at the Langmuir probe signals giving the integrated ion flux on the inner and outer divertor I_{in} and I_{out} (see Figure 5, upper curve), the asymmetries are more modest in all cases

(I_{in} / I_{out} in the range 2-4). It should be noted that translating the D_α signal in terms of particle flux is not trivial, as complex atomic processes, such as molecular dissociation or recombination, are to be taken into account, specially for partially detached plasmas. One should keep in mind that comparing directly the D_α signal from the attached outer divertor plasma, where a simple estimate should be valid (S/XB branching ratio around 20 ionizations per photons [6]) to the D_α signal from the often partially detached inner divertor is then difficult.

- Behaviour of the inner and outer divertor

Figure 6 presents the effect of outer and inner divertor gas puffing on the inner and outer divertor, for L mode discharges in the corner, lower and upper vertical configurations. The plasma volume averaged density is quite similar for the 3 configurations. The outer fuelling efficiency is seen to be lower than the inner fuelling efficiency, as the density reached with GIM11 is slightly higher, although the fuelling rate is 20% lower.

In the outer divertor, the 2 gas injections are clearly seen on the Langmuir probes and on the D_α signals (Figure 6 a), the D_α signal being the highest for the upper vertical position, where a large volume of the divertor is occupied by the private flux region. The 2 injections give about the same level of D_α and Langmuir probe signals, although the GIM11 injection is 20% lower.

In the inner divertor, the situation is more complex : the gas injection is barely seen on the ion flux, which even decreases during GIM11 injection, showing some evidence of detachment. The Dα signal increases strongly, except for the corner configuration with outer fuelling, where the gas injection is not seen, while it is the only case when it is seen on the Langmuir probe signal. The explanation is not clear at the moment, but this could correspond to a situation where the inner divertor plasma remains attached despite the gas injection.

Figure 6 b) presents the corresponding neutral pressures, measured in the main chamber, the private flux region and the subdivertor. Both injections are clearly seen on the pressure signals. The GIM11 injection leads to higher neutral pressures, although the fuelling rate is reduced compared to GIM9. The main chamber pressure is as expected much higher for the more open upper vertical configuration, where the divertor plasma plugging efficiency is reduced (in that case, this is not due to a direct leakage from the subdivertor into the main chamber, as outlined in [7], since the subdivertor pressure is lower for the upper vertical

configuration). The PFR pressure is increased with increasing the strike points height on the vertical plates. The subdivertor pressure is almost equivalent for the corner and lower vertical configurations, and remains significant even for the upper vertical configuration, where the strike points are quite far from the louvers (see section 3 for a discussion of the divertor particle exhaust).

- ELMs frequency

Last, for H mode discharges, the inner fuelling leads to a higher ELMs frequency for the same gas injection in the ITER like and the lower delta configurations, as was reported in [4] for the corner and vertical configurations (see Table 1).

3 Divertor particle exhaust efficiency

As we have seen in the previous section, the lowest wall retention is obtained in configurations where the divertor pumping is the most efficient. We will now take a closer look on the divertor performance in terms of particle exhaust. Figure 7 presents the evolution of the subdivertor neutral pressure and of the private flux region neutral pressure as a function of the plasma averaged density. In L mode (discharges with $<n_e>$ lower than $3.5\ 10^{19}\ m^{-3}$), the divertor pressure increases with density, which is a classical result already observed in several machines equipped with pumping systems. In H mode, for high density and partially detached plasmas, the pressure behaviour is more complex.

In all cases, the pressure is proportional to the particle flux entering the divertor louvers. From this obvious statement, we will try to derive a simple empirical law to estimate the subdivertor pressure. The experimental measurement chosen to represent the particle flux is the D_α signal integrated over the inner ($D\alpha_{in}$) and outer divertor ($D\alpha_{out}$) in photons/s. Indeed, Langmuir probes signal are not very well suited in situations where the particle flux is mainly composed of neutrals and not ions, such as plasma detachment or strong gas injection in the divertor. On the contrary, the D_α signal reflects ion recycling as well as gas injection or detached plasmas, although it should be taken with caution in the case of detached plasma (see comments in section 2.3.4). The integrated D_α value is then corrected by an attenuation factor, corresponding to the strike point location with respect to the louvers (f_{SPin} for the inner strike point, f_{SPout} for the outer strike point) : the further the strike point is from the louvers, the poorer is the pumping. The reference for the calculation of the attenuation factor is the

corner configuration, with the 2 strike points resting on the horizontal plates right in front of the louvers (R = 2.41 m Z = -1.73 m for the inner strike point, R = 2.91 m Z = -1.73 m for the outer strike point). By convention, the attenuation factor is taken to be 1 in this configuration of maximum pumping efficiency. Last, the divertor conductance has to be taken into account, as the divertor cryopump is located on the outer side of the divertor. A correction factor f_C, corresponding to the conductance difference between the inner and outer divertor, is applied to the inner particle flux. Finally, the subdivertor pressure can then be expressed as follows :

$$P_{subdiv} = k\,(f_{SPout}\,D\alpha_{out} + f_{SPin}\,f_C\,D\alpha_{in}) \qquad (2)$$

The proportionality factor k and the conductance factor f_C have been determined from a dedicated ohmic shot [9], where the strike points have been moved successively in and out from the throats, without moving the X point (see Figure 8). Four phases were programmed : both legs in throat, outer leg in throat only, both legs out, inner leg in throat only. As seen from Figure 8, even during the both legs up phase, with the strike points located more than 30 cm away from the reference corner configuration, the pressure measured in the subdivertor is still significant, indicating that the pumping is not only due to ballistic phenomena (direct collection of the incident ion flux through the louvers) but also to diffusive phenomena (indirect collection of the recycling neutrals reflected towards the louvers after several collisions with the divertor structure or the plasma). This effect has been clearly described in [8] and depends amongst other factors on the divertor geometry, which determines the neutral retention in the divertor volume. Moreover, one can also see in Figure 8 that the inner and outer contribution to pumping are of the same order when comparing the inner leg only and outer leg only phases : the asymmetry between the inner and the outer particle flux compensates for the conductance effect.

The factor k has been derived from the outer leg in the throat only phase, where one can assume $P_{subdiv} = k\,D\alpha_{out}$ (k = 5 for D_α in 10^{22} photons s^{-1} and P_{subdiv} in 10^{-3} mbar). The factor f_C has then been derived from the inner leg in throat only phase, where one can assume $P_{subdiv} = k\,f_C\,D\alpha_{in}$. The conductance factor is found to be around 0.35, in agreement with previous work [9]. Therefore, for a relatively modest asymmetry ($D\alpha_{in}$.= 3 $D\alpha_{out}$.which is often the case, specially with the MkIIGB divertor where asymmetries are more pronounced due to the septum [4]), the inner contribution to pumping is equivalent to the outer contribution if the 2 strike points are located at the same distance from the throats.

The value of k and f_C calculated above have then been used to derive the strike point correction factor f_{SP} for a variety of L mode discharges from the database described in section 2.2 with different magnetic configurations (corner, lower and upper vertical targets, high clearance 5 cm, high clearance 22 cm) and different fuelling locations (inner and outer divertor, main chamber). The results are shown in Figure 9, where the calculated strike points correction factors are represented as a function of the strike point distance along the vertical plate to the reference corner configuration. There is no significant difference between the inner and outer correction factors, which tends to confirm that the calculated value for the conductance factor f_C is correctly estimated. Moreover, one can see a sharp decrease in the correction factor as soon as the strike point moves away from the corner configuration (f_{SP} down to 0.4-0.5 for less than 5 cm), and then a smoother behaviour as the strike point is moved further away (f_{SP} finally down to 0.2-0.3 when the strike point is more than 20 cm away from the throat). The first sharp decrease can be attributed to the loss of the direct ballistic collection of the ion flux, the smoother behaviour would then correspond to the diffusive collection, which is still efficient even if the strike point is far from the throat, due to the significant closure of MkIIGB, which traps efficiently the neutral particles in the divertor region. Using the fit shown in Figure 9 for the strike points correction factor, equation (2) allows to reproduce the measured pressure within ± 20% for the L mode database in most configurations.

H mode discharges are more difficult to analyse, in particular due to the ELMs influence on the D_α signal; however, they show the same trend.

4 Summary and prospects

A particle balance analysis has been applied to a variety of L mode and H mode discharges of the C4 campaign, in different magnetic configurations and with different divertor gas puffing location. A few tens of seconds after the end of the discharge, the dynamic wall retention is found to be around 60% of the injected flux, while the divertor extracts from 20-30 up to 40-50 % of the injected flux, depending on the plasma configuration (the rest is extracted by the vessel pumping system). The lowest wall retention (50%) is obtained with the corner and the lower delta configuration in H mode, where the divertor pumping is the most efficient, while the ITER like configuration is less favourable. However, it should be reminded that besides

the strong dynamic wall retention, the overall long term wall retention integrated on the C1-C4 campaigns is found to be around 8%, within 10% error bars [2], as the wall releases particles between shots.

When comparing similar shots with different wall temperature (T_{wall} = 200 °C during the C4 campaign instead of 320 °C during previous campaigns), the wall retention is found to be slightly higher with the cold wall temperature (60 % instead of 50 %). The wall temperature also seems to affect the ELMs frequency for moderate gas fuelling (increased f_{ELM} at lower T_{wall}), but the effect disappears for low and strong gas fuelling.

The influence of the gas puffing location is more difficult to analyse. In most configurations, outer gas injection leads to a lower plasma fuelling efficiency and a higher wall retention. In all cases, strong asymmetries are observed between the inner and outer divertor for MkIIGB : $D\alpha_{in}$ is always stronger than $D\alpha_{out}$, even when gas puffing is performed from the outer divertor. However, the level of asymmetry can be reduced with outer fuelling in closed divertor configurations, such as the corner configuration. Last, inner fuelling seems to lead to higher ELMs frequency.

The pumping performance of the divertor has been studied : the pressure in the divertor can be expressed as a linear function of the integrated Dα signals $D\alpha_{in}$ and $D\alpha_{out}$ and a correction factor to take into account the position of the strike points with respect to the louvers. The inner leg contribution to pumping is found to be important for MkIIGB, because the strong in/out asymmetry in the particle flux compensates for the conductance effect.

Further work will address particle balance analysis, using the same methodology as described here, applied to Tore Supra, which operates at T_{wall} = 150°C, and in which the importance of the wall contribution has already been clearly identified in long pulse experiments [10].

References :

[1] : P. Andrew et al., J. Nucl. Mater. 266-269 (1999) 153

[2] : J. Bucalossi et al., « Particle Balance studies in JET », to be published in Proc. 28th Eur. Phys. Soc. Conf. on Controlled Fusion and Plasma Physics, Madeira, (2001)

[3] : J. Rapp et al., « Effect of wall temperature and divertor closure on the L mode density limit at JET », to be published in Proc. 28th Eur. Phys. Soc. Conf. on Controlled Fusion and Plasma Physics, Madeira, (2001)

[4] : C. Maggi et al., Proc. 26th Eur. Phys. Soc. Conf. on Controlled Fusion and Plasma Physics, Maastricht, Vol. 23J, European Physical Society (1999) 201.

[5] : M. Bécoulet, " ELMs on JET at different vessel temperature", private communication

[6] : A. Pospieszczyk, *Atomic & Plasma-Material Interaction Processes in Controlled Thermonuclear Fusion*, R. Janev & H. Drawin éd., *Elsiever Science Publishers* (1993) p215

[7] : C. S. Pitcher, "Main chamber neutral pressure in Alcator C mod and JET", to be published in Proc. 28th Eur. Phys. Soc. Conf. on Controlled Fusion and Plasma Physics, Madeira, (2001)

[8] : A. Loarte, "Effect of divertor geometry on tokamak plasmas", Plasma Phys. Control. Fusion, 43 (2001), R183-R224

[9] : A. Loarte, private communication (presentation to the general design review meeting of the JET EP project, 25/26 july 2000, which can be found in the JET users page http://users.jet.efda.org/pages/jet-ep/designreview0700/edge2d-div-pumping.pdf)

[10] : C. Grisolia et al., J. Nucl. Mater. 266-269 (1999) 146

List of figure captions

- Table 1 : Comparison of hot walls and cold walls discharges in 2 magnetic configurations for medium gas fuelling (ELM frequency f_{ELM} in Hz, plasma volume averaged density <ne> in 10^{19} m^{-3}, private flux region and subdivertor pressure p_{PFR} and p_{subdiv} in 10^{-3} mbar)
- Figure 1 : Comparison of the different magnetic configurations. The reference corner configuration is drawn in blue.
- Figure 2 : Location of the different divertor gas injection points used in the present study (GIM6, which is a main chamber mid plane fuelling valve is not shown here). They are shown with 2 different magnetic configurations (ITER like above, lower delta below) to illustrate that the same GIM can lead to fuel either the scrape off layer or the private flux region, depending on the magnetic configuration.
- Figure 3 : Fraction of injected particles extracted by the divertor (stars) and retained in the wall (circles) as a function of the subdivertor neutral pressure for the studied database. The trends for the divertor fraction and the wall fraction are suggested with the dashed lines (respectively orange and purple), only drawn to guide the eye of the reader.
- Figure 4 : Comparison of ELMs frequency as a function of the gas fuelling for hot walls (Twall = 320°C in red) and cold walls (Twall = 200 °C, C4 campaign in black) in the ITER like configuration [5]
- Figure 5 : Particle flux in/out asymmetry for the MkIIGB divertor as a function of the averaged plasma density for a variety of L mode (<ne> lower than 3.5 1019 m-3) and H mode (<ne> larger than 5 1019 m-3) discharges in different magnetic configurations. Gas puffing locations are also varied. Above : in/out asymmetry in the ion flux signal (ratio of the ion flux integrated on the inner divertor Isatin over the ion flux integrated on the outer divertor Isatout). Below : in/out asymmetry in the D_ signal (ratio of the D_ signal integrated on the inner divertor D_in over the D_ signal integrated on the outer divertor D_out). D_in / D_out = 1 and Isatin / Isatout = 1 are indicated in black.
- Figure 6 : Effect of divertor gas puffing for L mode discharges in different magnetic configurations with decreasing divertor closure : corner, lower and upper vertical configurations. 2 successive gas puff are performed : the first from the outer divertor (GIM9), the second from the inner divertor (GIM11).
- Figure 7 : Subdivertor and private flux region (PFR) neutral pressure as a function of the plasma averaged density for a variety of L mode (<ne> lower than 3.5 1019 m-3) and H mode (<ne> larger than 5 1019 m-3) discharges in different magnetic configurations for the MkIIGB divertor.
- Figure 8 : Time evolution of the D_ signal integrated over the inner divertor (D_in in red) and the outer divertor (D_out in blue) and the corresponding subdivertor pressure (in green) during a sequence where the strike points were successively moved in and out from the divertor throats.
- Figure 9 : Calculated strike point correction factor for the inner and outer divertor as a function of the distance of the strike points to the reference corner configuration for different L mode discharges.

Lower delta	f_{ELM}	$<n_e>$	p_{PFR}	p_{subdiv}	ITER like	f_{ELM}	$<n_e>$	p_{PFR}	p_{subdiv}
53048 GIM9	50	7.1	4.5	2.2	53041 GIM9	25	8	2.8	1.5
53050 GIM10	45	7.5	5.8	2.5	53039 GIM10	22	8.3	2.7	1.3
53047 GIM11	66	7.6	8.6	3.5	53043 GIM11	37	8.2	4.6	2.2
52823 GIM11 hot walls	54	9.2	15	3.6	52783 GIM11 hot walls	23	9.2	9.3	2.6

Table 1 : Comparison of hot walls and cold walls discharges in 2 magnetic configurations for medium gas fuelling (ELM frequency f_{ELM} in Hz, plasma volume averaged density <ne> in 10^{19} m^{-3}, private flux region and subdivertor pressure p_{PFR} and p_{subdiv} in 10^{-3} mbar)

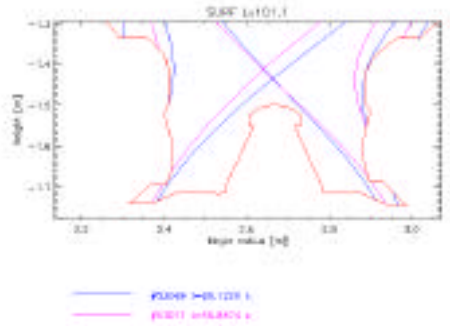 Corner configuration (in blue) and high clearance 5 cm configuration (in magenta)	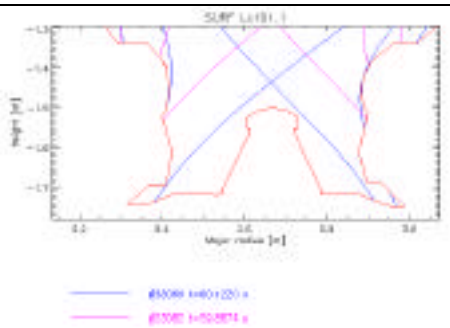 Corner configuration (in blue) and high clearance 22 cm configuration (in magenta)
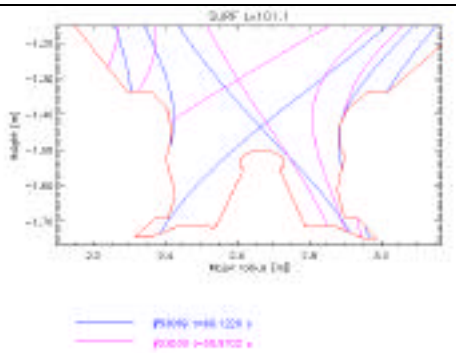 Corner configuration (in blue) and ITER like configuration (in magenta)	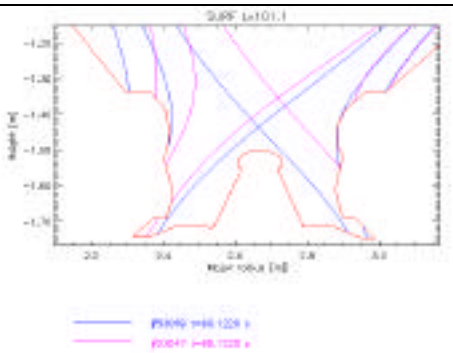 Corner configuration (in blue) and lower delta configuration (in magenta)
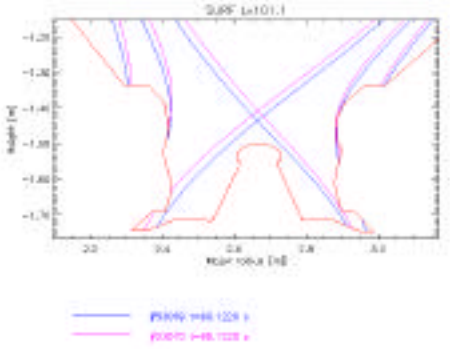 Corner configuration (in blue) and lower vertical configuration (in magenta)	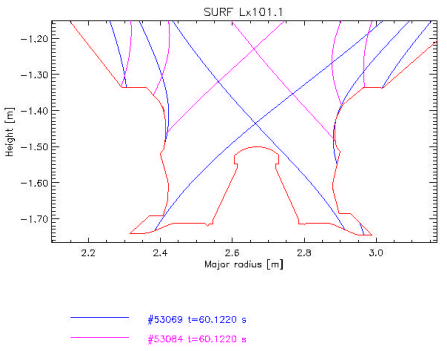 Corner configuration (in blue) and upper vertical configuration (in magenta)

Figure 1 : Comparison of the different magnetic configurations. The reference corner configuration is drawn in blue.

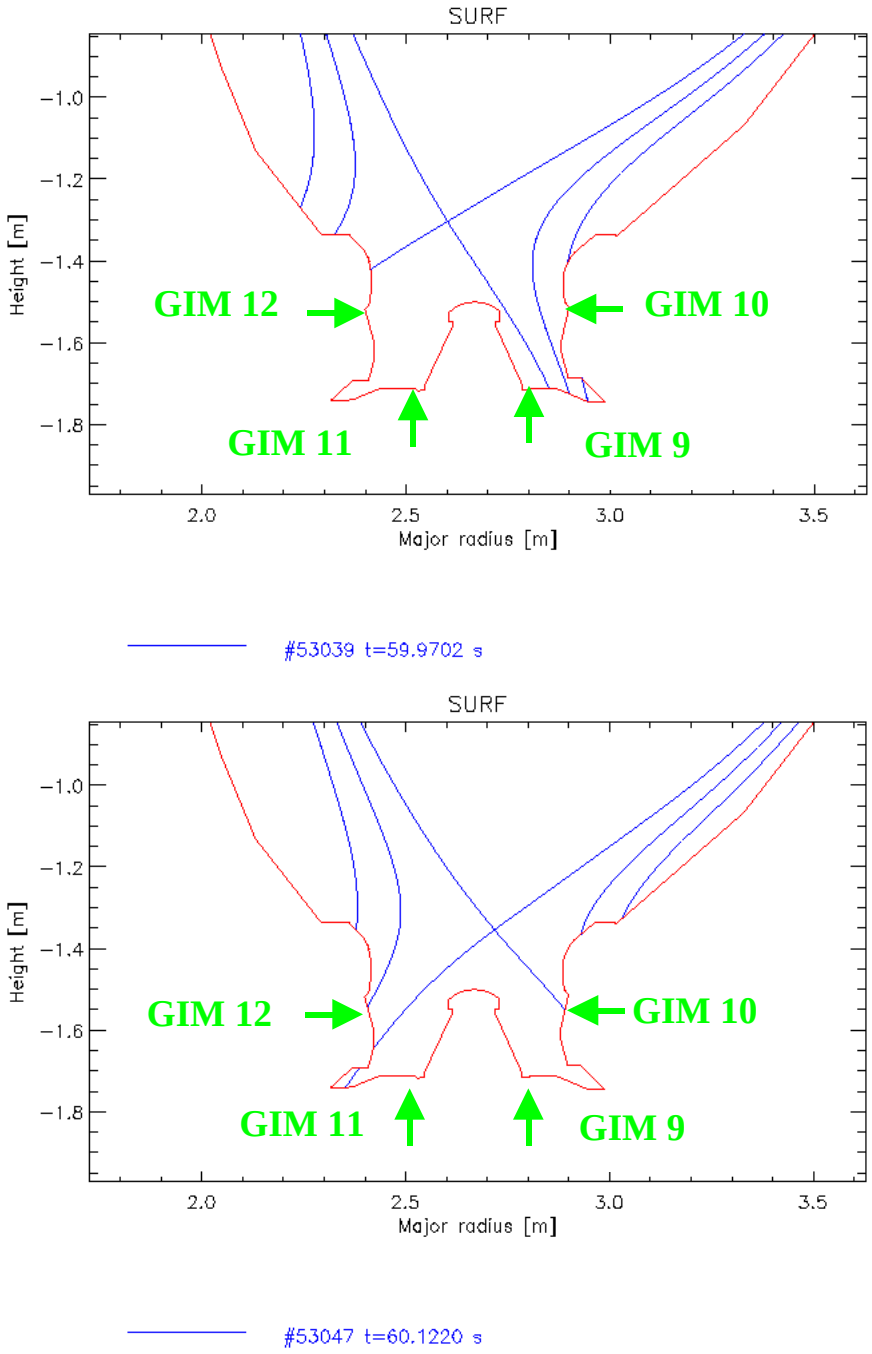

Figure 2 : Location of the different divertor gas injection points used in the present study (GIM6, which is a main chamber mid plane fuelling valve is not shown here). They are shown with 2 different magnetic configurations (ITER like above, lower delta below) to illustrate that the same GIM can lead to fuel either the scrape off layer or the private flux region, depending on the magnetic configuration.

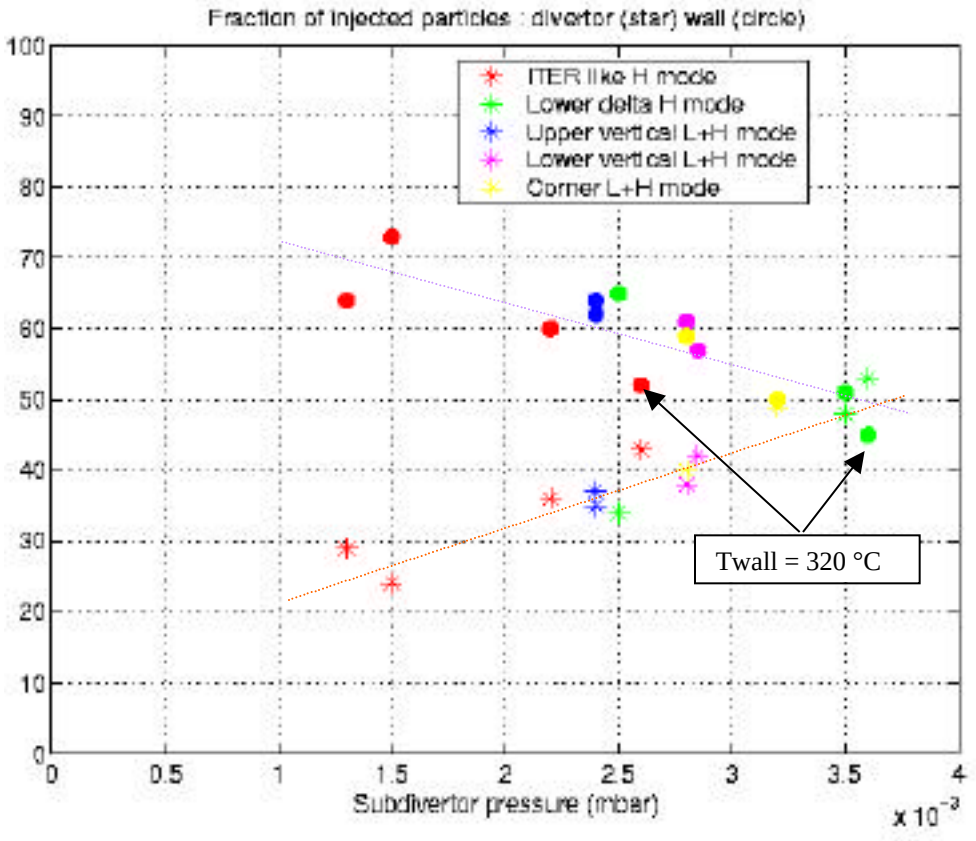

Figure 3 : Fraction of injected particles extracted by the divertor (stars) and retained in the wall (circles) as a function of the subdivertor neutral pressure for the studied database. The trends for the divertor fraction and the wall fraction are suggested with the dashed lines (respectively orange and purple), only drawn to guide the eye of the reader.

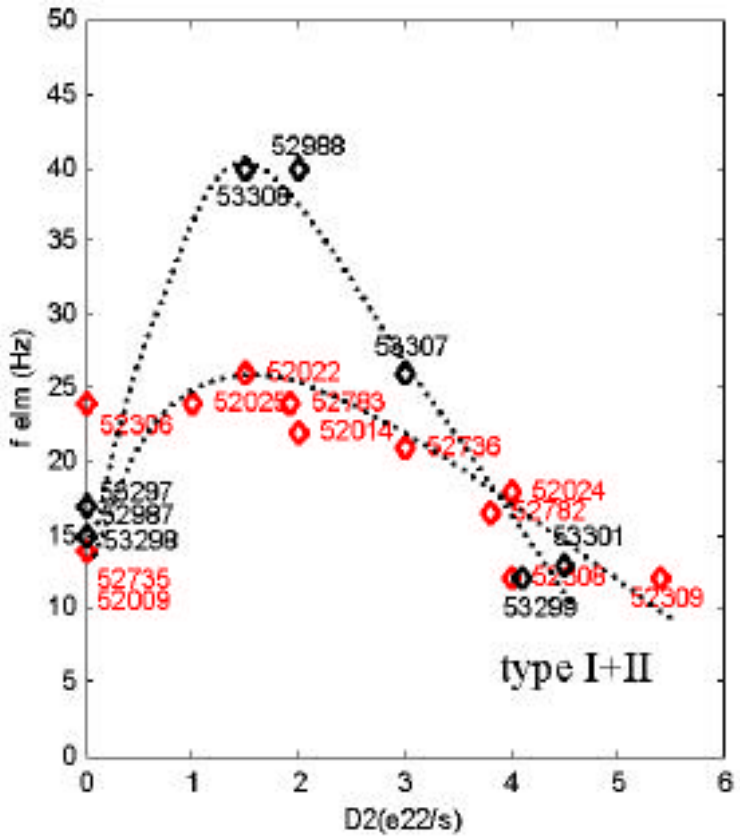

Figure 4 : Comparison of ELMs frequency as a function of the gas fuelling for hot walls (T_{wall} = 320°C in red) and cold walls (T_{wall} = 200 °C, C4 campaign in black) in the ITER like configuration [5]

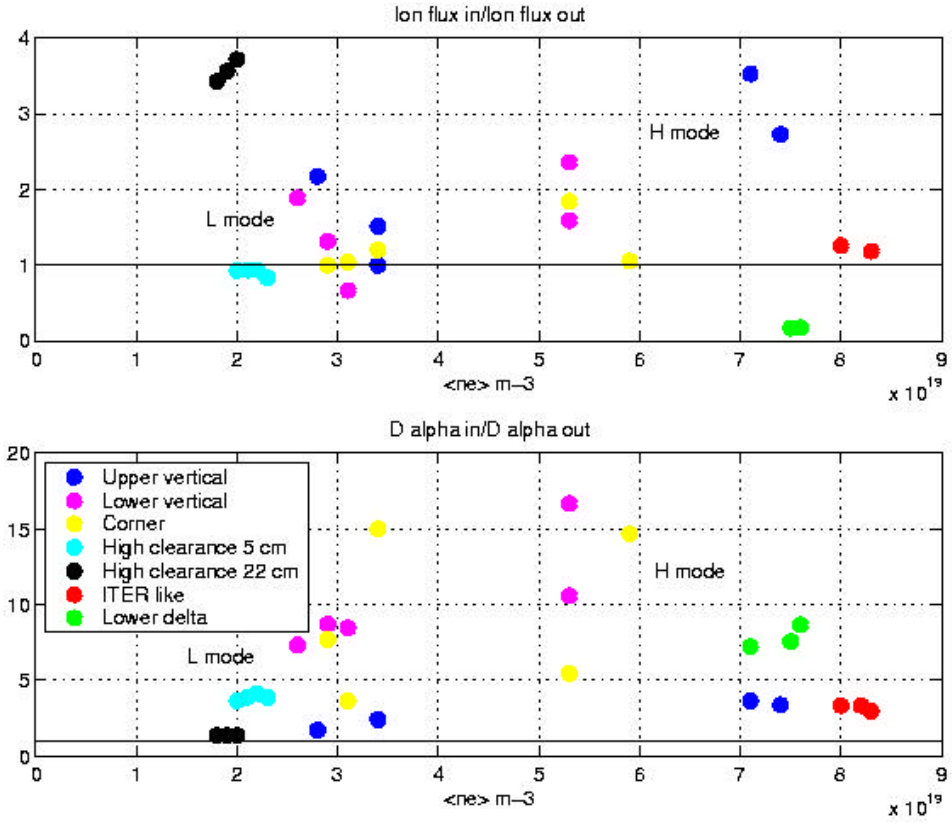

Figure 5 : Particle flux in/out asymmetry for the MkIIGB divertor as a function of the averaged plasma density for a variety of L mode (<n_e> lower than 3.5 10^{19} m^{-3}) and H mode (<n_e> larger than 5 10^{19} m^{-3}) discharges in different magnetic configurations. Gas puffing locations are also varied. Above : in/out asymmetry in the ion flux signal (ratio of the ion flux integrated on the inner divertor $Isat_{in}$ over the ion flux integrated on the outer divertor $Isat_{out}$). Below : in/out asymmetry in the Dα signal (ratio of the Dα signal integrated on the inner divertor $D\alpha_{in}$ over the Dα signal integrated on the outer divertor $D\alpha_{out}$). $D\alpha_{in}$ / $D\alpha_{out}$ = 1 and $Isat_{in}$ / $Isat_{out}$ = 1 are indicated in black.

6a)

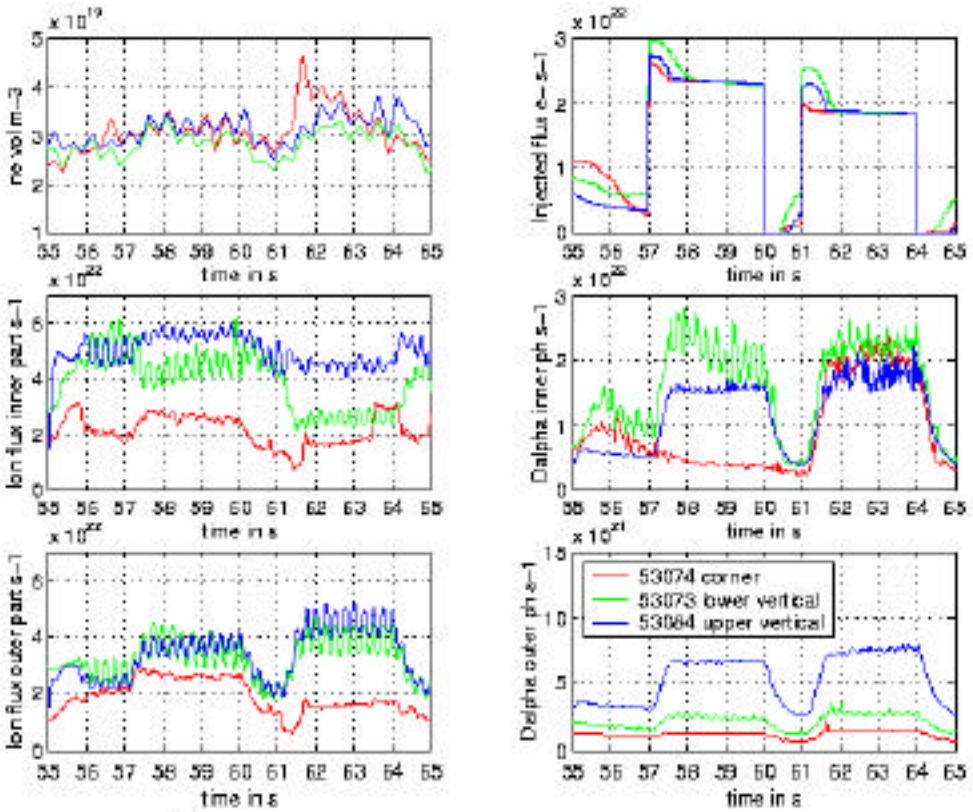

6b)

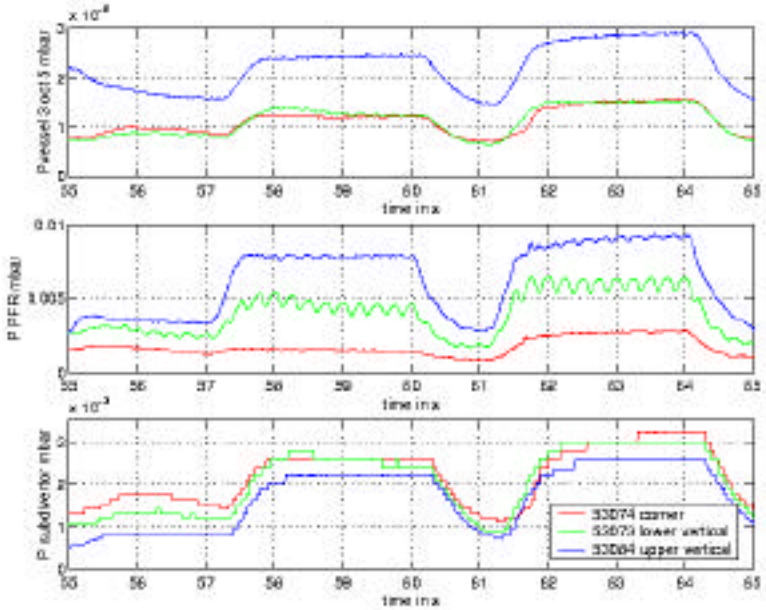

Figure 6 : Effect of divertor gas puffing for L mode discharges in different magnetic configurations with decreasing divertor closure : corner, lower and upper vertical configurations. 2 successive gas puff are performed : the first from the outer divertor (GIM9), the second from the inner divertor (GIM11).
6a) From the top on the left column : plasma averaged density, ion flux integrated on the inner divertor, ion flux integrated on the outer divertor. From the top on the right column : gas puff sequence, D_α signal integrated on the inner divertor, D_α signal integrated on the outer divertor.
6b) neutral pressure measured in the main chamber (top), in the private flux region (middle) and in the subdivertor (below)

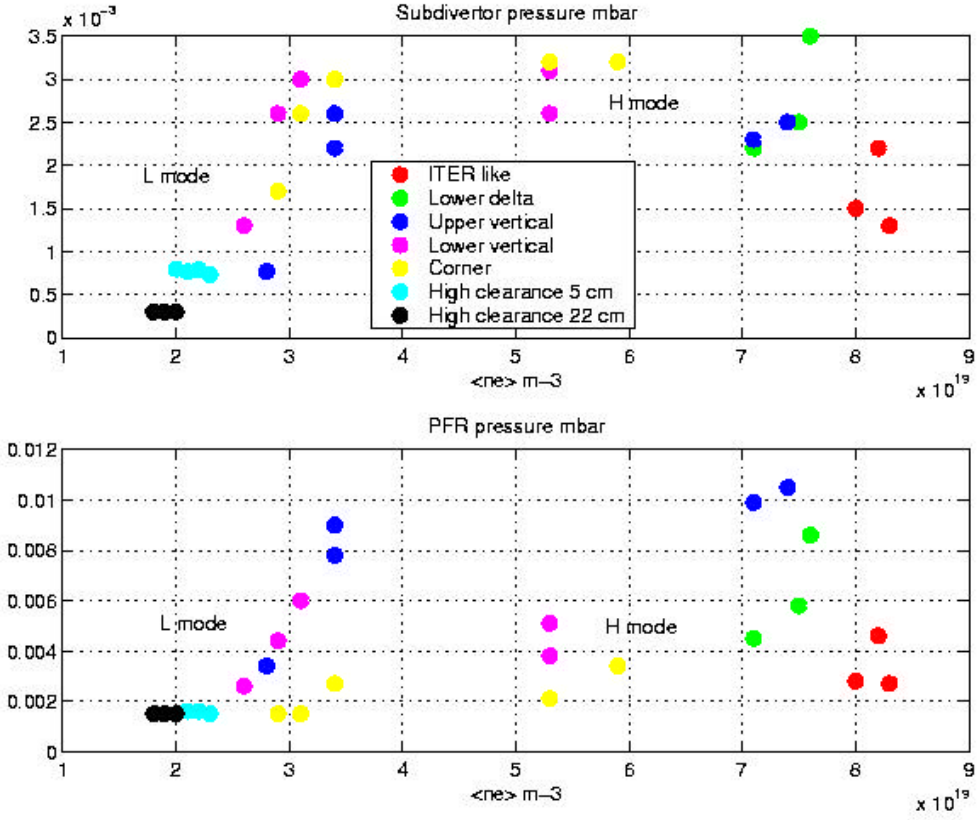

Figure 7 : Subdivertor and private flux region (PFR) neutral pressure as a function of the plasma averaged density for a variety of L mode (<n_e> lower than 3.5 10^{19} m^{-3}) and H mode (<n_e> larger than 5 10^{19} m^{-3}) discharges in different magnetic configurations for the MkIIGB divertor.

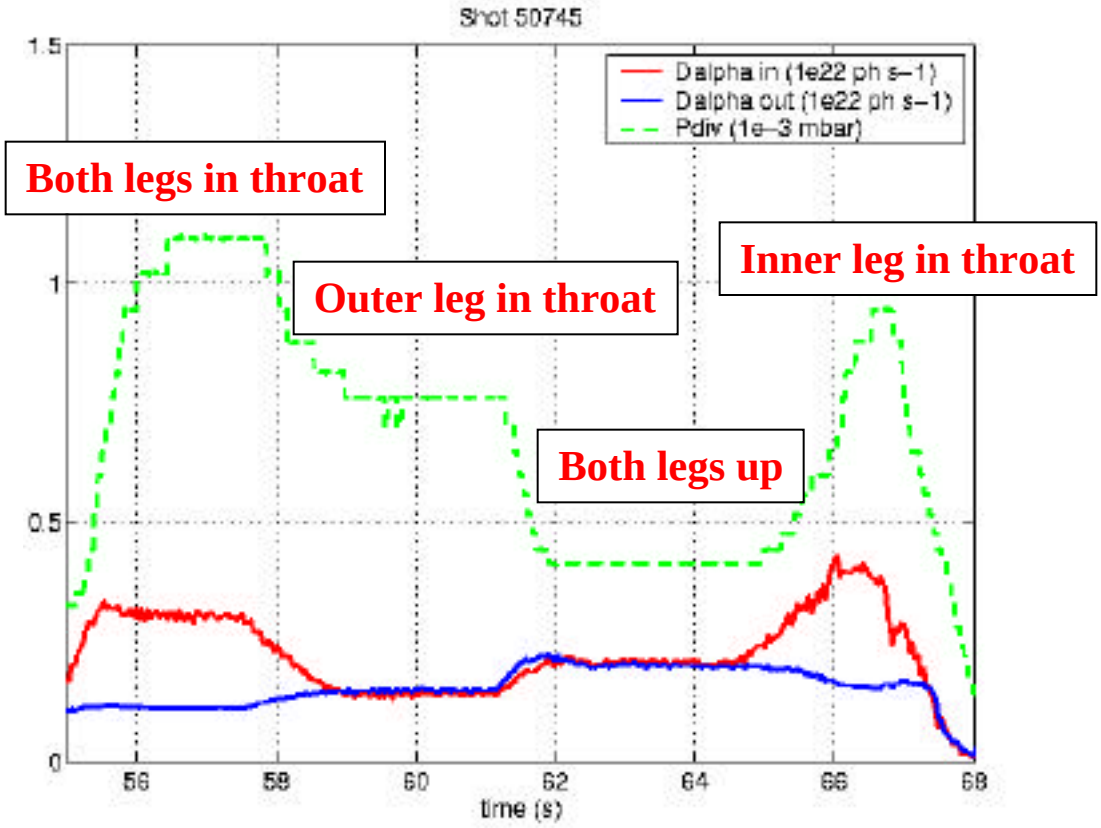

Figure 8 : Time evolution of the Dα signal integrated over the inner divertor ($D\alpha_{in}$ in red) and the outer divertor ($D\alpha_{out}$ in blue) and the corresponding subdivertor pressure (in green) during a sequence where the strike points were successively moved in and out from the divertor throats.

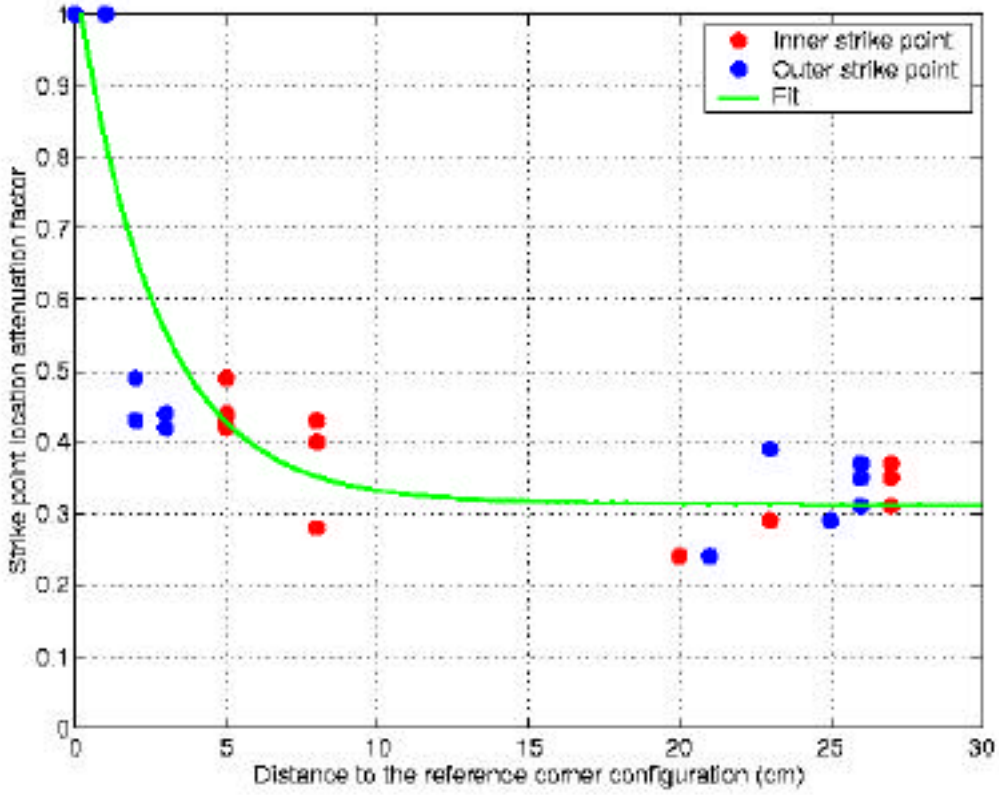

Figure 9 : Calculated strike point correction factor for the inner and outer divertor as a function of the distance of the strike points to the reference corner configuration for different L mode discharges. The green line represents the fit used to calculate the subdivertor pressure from equation (2).